

# Injectable Electroactive Hydrogels Formed via Host–Guest Interactions

Yaobin Wu,<sup>†</sup> Baolin Guo,<sup>\*,†</sup> and Peter X. Ma<sup>\*,†,‡,§,||,⊥</sup>

<sup>†</sup>Center for Biomedical Engineering and Regenerative Medicine, Frontier Institute of Science and Technology, Xi'an Jiaotong University, Xi'an, 710049, China

<sup>‡</sup>Department of Biomedical Engineering, University of Michigan, Ann Arbor, Michigan 48109, United States

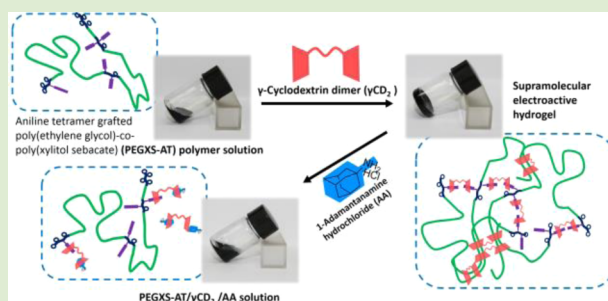
<sup>§</sup>Department of Biologic and Materials Sciences, University of Michigan, 1011, North University Avenue, Room 2209, Ann Arbor, Michigan 48109, United States

<sup>||</sup>Macromolecular Science and Engineering Center, University of Michigan, Ann Arbor, Michigan 48109, United States

<sup>⊥</sup>Department of Materials Science and Engineering, University of Michigan, Ann Arbor, Michigan 48109, United States

## S Supporting Information

**ABSTRACT:** Injectable conducting hydrogels (ICHs) are promising conductive materials in biomedicine and bioengineering fields. However, the synthesis of ICHs in previous work involved chemical cross-linking, and this may result in biocompatibility problems of the hydrogels. We present the successful synthesis of ICHs via noncovalent host–guest interactions, avoiding the side effect of covalent chemical cross-linking. The ICHs are based on the  $\gamma$ -cyclodextrin dimer as the host molecule and tetraaniline and poly(ethylene glycol) as the guests in a synthetic well-defined hydrophilic copolymer. The sol–gel transition mechanism of the in situ hydrogel is thoroughly investigated. This novel synthesis approach of ICHs via supramolecular chemistry will lead to various new biomedical applications for conducting polymers.



Electrically conducting polymers (ECPs), such as polythiophene, polypyrrole, polyaniline (PANI), and their derivatives, have attracted great attention in recent years.<sup>1–4</sup> Among these diverse ECPs, PANI is very eminent because of its excellent combination of environmental stability, controllability, and simple synthesis.<sup>5–7</sup> However, the hydrophobicity, infusibility, and lack of degradability of PANI greatly restricted its practical biomedical applications.<sup>8,9</sup> By combining the advantages of conducting polymers and hydrogels, electrically conducting hydrogels have been recently developed to overcome these drawbacks.<sup>10–15</sup> For instance, a single component conducting polymer hydrogel based on poly(3-thiopheneacetic acid) which was covalently cross-linked with 1,1'-carbonyldiimidazole was developed.<sup>16</sup> The conducting hydrogels supported the cell adhesion and proliferation of fibroblast and myoblast cells and showed all the requisite hydrogel characteristics as scaffold materials. Electrically conductive composite hydrogels composed of oligo-(polyethylene glycol) fumarate (OPF) and polypyrrole were prepared for applications in nerve regeneration.<sup>17</sup> PC12 cells showed significantly higher cell attachment and an increase in the percentage of neurite bearing cells on OPF/polypyrrole hydrogels compared to that on OPF. The conducting hydrogels with tunable swelling ratios and conductivity based on chitosan and aniline oligomers were prepared by chemical cross-linking

for tissue engineering application.<sup>18,19</sup> However, the surgical intervention for *in vivo* implantation of these preshaped conducting hydrogels is inevitable. Therefore, the injectable conducting hydrogels have been developed by our group.<sup>20</sup> A series of injectable electroactive hydrogels were synthesized by in situ chemical cross-linking of gelatin-*graft*-polyaniline by genipin under physiological conditions.<sup>20</sup> The conductivity of the swollen conductive hydrogels was in the range of  $10^{-4}$  S/cm, and these injectable conductive hydrogels greatly enhanced the adhesion and proliferation of mesenchymal stem cells and C2C12 myoblast cells. This work opens the way to developing injectable conducting hydrogels for tissue regeneration applications. However, chemical gelation for injectable conducting hydrogels usually involves the residual initiators or monomers or cross-linker in the hydrogel matrix, and these cross-linking agents such as glutaraldehyde, polyepoxides, and isocyanate are usually highly toxic and easily leach into the body during the cross-linking processing.<sup>21–23</sup> Therefore, the biocompatibility of conducting hydrogels with chemical cross-linking is still a challenge in the use of these materials as injectable hydrogels.<sup>24,25</sup> In contrast, the physically cross-linked

Received: August 14, 2014

Accepted: October 14, 2014

Published: October 17, 2014

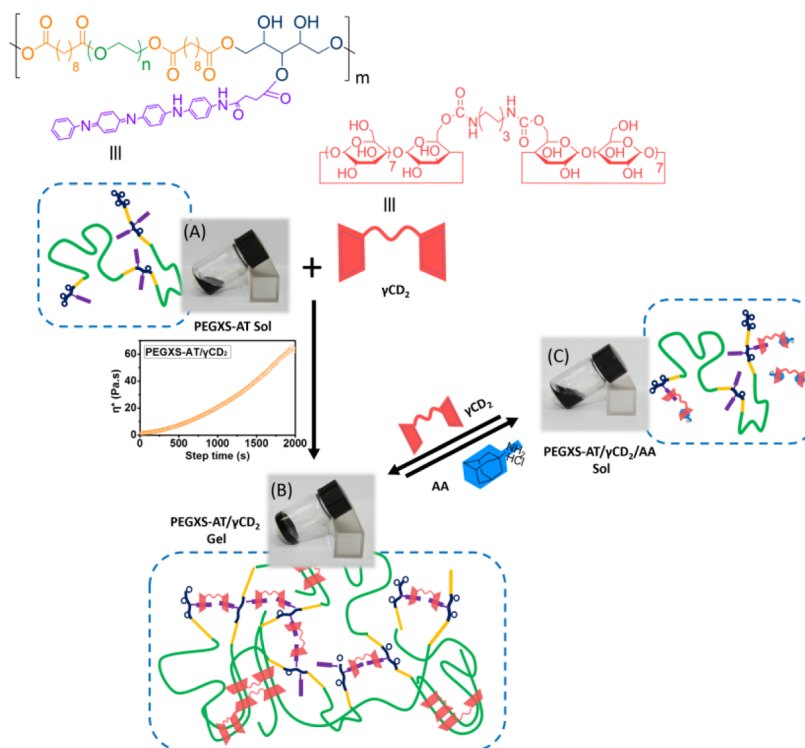


**Figure 1.**  $\gamma$ -Cyclodextrin dimer host ( $\gamma\text{CD}_2$ ) and guest copolymer (PEGXS-AT) and formation of injectable electroactive hydrogel via host–guest interaction between CD units with PEG and AT segments. The reversible sol–gel transition was achieved by subsequent alternation via addition of 1-adamantanamine hydrochloride (AA) and  $\gamma\text{CD}_2$  into the mixture.

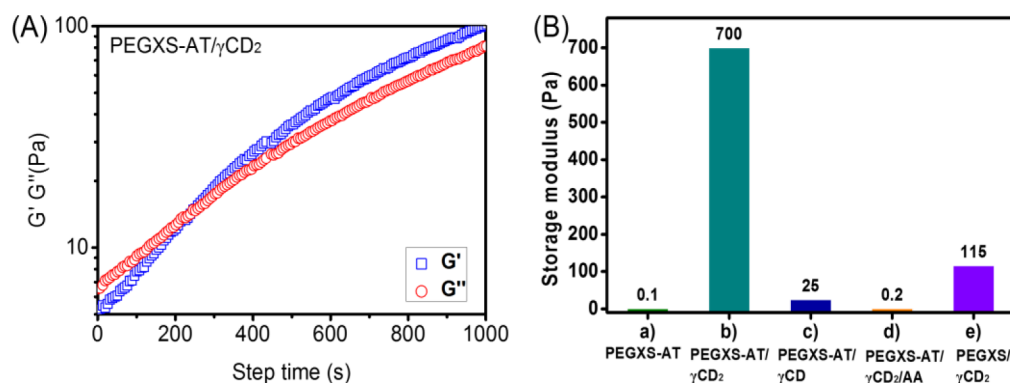


**Figure 2.** Rheological assay of mixtures. (A) The rheological step time analysis of the PEGXS-AT/ $\gamma\text{CD}_2$  mixture. (B) The storage modulus ( $G'$ ) of (a) PEGXS-AT sol, (b) PEGXS-AT/ $\gamma\text{CD}_2$  gel, (c) PEGXS-AT/ $\gamma\text{CD}$  sol, (d) PEGXS-AT/ $\gamma\text{CD}_2$ /AA sol, and (e) PEGXS/ $\gamma\text{CD}_2$  gel.

hydrogels with no covalent cross-linking have several advantages over chemically cross-linked hydrogels because they do not require any cross-linking agents for the gelation and do not release heat during polymerization *in situ*, and furthermore the mild gelation processing would not denature incorporated proteins and damage embedded cells and surrounding tissues at the gelation site.<sup>23,26</sup>

Supramolecular hydrogels prepared by noncovalent host–guest interactions have been reported and attracted increased attention recently.<sup>27–30</sup> Cyclodextrins (CDs) have been the most widely used as the host molecules in the supramolecular hydrogel system,<sup>31–36</sup> and many reversible supramolecular systems based on CDs have been established.<sup>37–39</sup> However, there is no report about design and synthesis of injectable conducting hydrogels via the noncovalent supramolecular interaction between conducting polymers and cyclodextrins.

The aim of this work is to synthesize novel injectable degradable conducting hydrogels formed via noncovalent host–guest interactions. The  $\gamma$ -cyclodextrin dimer ( $\gamma\text{CD}_2$ ) with good water solubility was selected as a host unit, while a synthetic well-defined hydrophilic copolymer (PEGXS-AT) based on PEG and aniline oligomer segments was employed as the guest component (Figure 1). The formation mechanism of these injectable conducting hydrogels was further investigated. The host–guest interactions between  $\gamma\text{CD}_2$  with PEG and aniline tetramer (AT) are the driving forces for the formation of the injectable conducting hydrogels. This work opens new ways to synthesize injectable conducting hydrogels via noncovalent interaction and leads to new biomedical applications of these conducting hydrogels.

The guest copolymer (PEGXS-AT) (Figure 1) containing PEG and aniline tetramer was prepared via two stages. In brief, the first stage consisted of the synthesis of PEGXS polymer by

polycondensation of PEG, sebacic acid, and xylitol and the synthesis of carboxyl-capped aniline tetramer (AT) (Schemes S1 and S2 in the Supporting Information). In the second stage, the AT segments were grafted onto the PEGXS polymer chain to obtain the PEGXS-AT copolymer (Scheme S3 in the Supporting Information). On the other hand, the host molecule  $\gamma$ CD dimer ( $\gamma$ CD<sub>2</sub>) was prepared from  $\gamma$ CD by reacting with hexamethylene diisocyanate (HDI) (Figure 1 and Scheme S4 in the Supporting Information). The chemical structure of the PEGXS-AT copolymer and  $\gamma$ CD<sub>2</sub> was confirmed by <sup>1</sup>H NMR and FT-IR spectra (Figure S1 and Figure S2 in the Supporting Information). When the mixture of PEGXS-AT aqueous solution (27 wt %) and  $\gamma$ CD<sub>2</sub> aqueous solution (10 wt %) was mixed and then ultrasonicated for 10 min, the viscosity of the mixture first increased and then transformed into a gel (Figure 1(A),(B)). The time sweep rheological assay showed that the storage modulus ( $G'$ ) became higher than the loss modulus ( $G''$ ) after assaying for about 265 s. The crossover point between  $G'$  and  $G''$  implied the sol-to-gel transition for the PEGXS-AT/ $\gamma$ CD<sub>2</sub> mixture (Figure 2(A)). To clarify the formation mechanism of these hydrogels, the sol-gel transition and mechanical properties of the other mixture systems were investigated (Table S1 in the Supporting Information). The PEGXS-AT sol (27 wt %) showed a higher  $G''$  than  $G'$  during the test period, which indicated that the PEGXS-AT sol did not form hydrogel (Figure S3(A) and Figure S4(A) in the Supporting Information), and PEGXS-AT/ $\gamma$ CD<sub>2</sub> hydrogel showed much higher  $G'$  than that of the PEGXS-AT sol (Figure 2(B)). Subsequently, when the excess molar amounts of AA to  $\gamma$ CD<sub>2</sub> (PEGXS-AT/ $\gamma$ CD/AA = 27 wt %/10 wt %/5 wt %) were added into the hydrogel and then treated by ultrasound processing, the gel turned into a sol in a few minutes (Figure S3(C) in the Supporting Information), and the  $G'$  decreased from 700 Pa into 0.2 Pa after gel-to-sol transition (Figure 2(B)). Furthermore, PEGXS-AT/ $\gamma$ CD<sub>2</sub>/AA sol went into a gel again after adding excess  $\gamma$ CD<sub>2</sub> into the mixture (Figure 1(B) (C)). For PEGXS-AT/ $\gamma$ CD (27 wt %/10 wt %) mixture, the viscosity and  $G'$  increased after adding  $\gamma$ CD into the PEGXS-AT solution, however the mixture still presented the solution state (Figure S3 (D) in the Supporting Information). In addition, PEGXS/ $\gamma$ CD<sub>2</sub> (27 wt %/10 wt %) mixture also exhibited the sol-gel transition (Figure S3 (F) and Figure S4 (B) in the Supporting Information). However, this gel showed the lower mechanical properties ( $G'$ ) and the higher equilibrated swelling ratio than those of PEGXS-AT/ $\gamma$ CD<sub>2</sub> gel (Figure 2 (B) and Figure S5 in the Supporting Information), which indicates that both PEGXS polymer chain and AT segments could interact with  $\gamma$ CD<sub>2</sub> host molecules and the interactions between PEGXS-AT and  $\gamma$ CD<sub>2</sub> make an important contribution to this supramolecular hydrogel formation. Furthermore, when PEGXS-AT/ $\gamma$ CD<sub>2</sub> mixture was treated with ultrasonication, it shows a shorter gelation time and a higher storage modulus ( $G'$ ) compared with the gels without ultrasonication treatment (Figure S6 and Figure S7 in the Supporting Information), which suggests that ultrasonication could make the assemble interaction between PEGXS-AT and  $\gamma$ CD<sub>2</sub> more rapidly and effectively. On the other hand, the other ratio mixtures of PEGXS-AT/ $\gamma$ CD<sub>2</sub> were also prepared and the rheological properties were investigated (Table S2 in the Supporting Information). As shown in Figure S8 in the Supporting Information, it was observed that the PEGXS-AT/ $\gamma$ CD<sub>2</sub> hydrogel were formed when the concentrations of mixtures were higher than PEGXS-AT  $\geq$ 15 wt %

and  $\gamma$ CD<sub>2</sub>  $\geq$ 10 wt %. In addition, the storage modulus ( $G'$ ) of mixtures increased from 50 to 1500 Pa when the PEGXS-AT concentration increased from 15 wt % to 45 wt % (Figure S9 in the Supporting Information). These results indicate that both the concentrations of PEGXS-AT and  $\gamma$ CD<sub>2</sub> play a critical role in the mixtures gelation and hydrogel mechanical properties.

As the lack of studies on host-guest interaction between CDs and aniline oligomers, in this work, we used  $\gamma$ CD and AT as model molecules to investigate the supramolecular interaction mechanism between them. <sup>1</sup>H NMR studies and UV analysis provided important insight into the physical interaction between  $\gamma$ CD and AT and the mechanism of hydrogel formation. Compared with AT and  $\gamma$ CD molecule, the <sup>1</sup>H NMR spectra of AT/ $\gamma$ CD showed remarkable changes; that is, the aromatic proton signals of AT units shifted to a lower field and the proton signals of H-3, H-5, and H-6 in  $\gamma$ CD to a higher field, indicating that AT molecules were inserted into the cavities of  $\gamma$ CD molecules (Figure 3, and Figure S10(B) in the

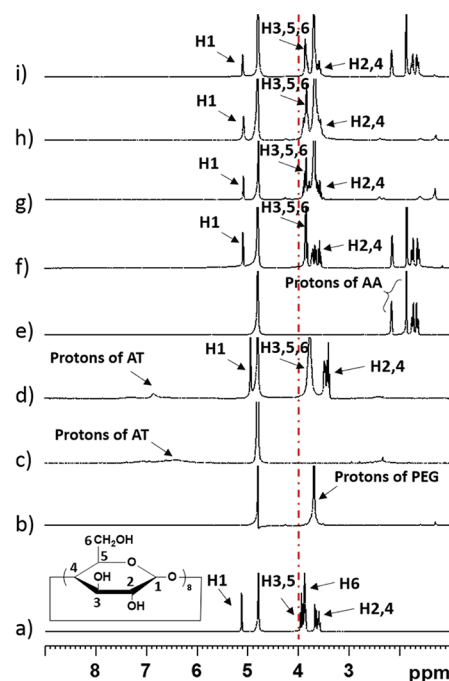


**Figure 3.** <sup>1</sup>H NMR spectra of (a)  $\gamma$ CD, (b) PEGXS-AT, (c) AT, (d) AT/ $\gamma$ CD, (e) AA, (f) AA/ $\gamma$ CD, (g) PEGXS/ $\gamma$ CD, (h) PEGXS-AT/ $\gamma$ CD, and (i) PEGXS-AT/ $\gamma$ CD/AA solution in D<sub>2</sub>O.

Supporting Information). These results are consistent with the interaction between CDs with other guest molecules in the literature.<sup>40</sup> The UV spectra of both AT and AT/ $\gamma$ CD showed two absorbance peaks at about 306 and 550–590 nm, which are attributed to the  $\pi$ - $\pi^*$  transition of the benzene ring and benzenoid (B) to quinoid (Q)  $\pi_B$ - $\pi_Q$  excitonic transition. Obviously, the Q/B absorbance peak of the AT/ $\gamma$ CD mixture showed a remarkable red shift compared with that of AT, which also suggested the formation of the host-guest interaction between  $\gamma$ CD and AT according to the phenomena of inclusion interaction between PANI with CDs.<sup>41</sup> Interestingly, the AT/ $\beta$ CD mixture also showed a slight red shift of the Q/B peak, whereas the AT/ $\alpha$ CD mixture did not (Figure S11 in the Supporting Information), indicating that the cavity of  $\beta$ CD or  $\gamma$ CD is large enough to encapsulate the AT molecule compared with  $\alpha$ CD. Furthermore, the addition of AA, as competitive



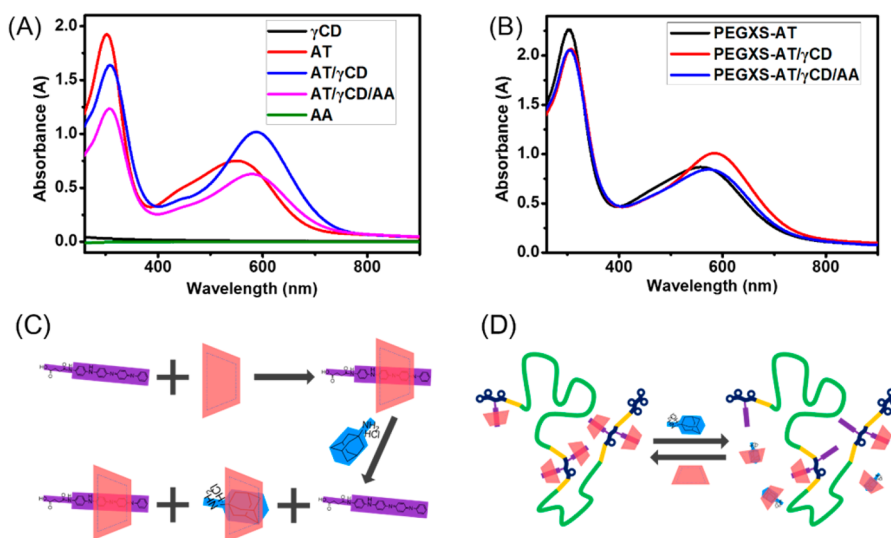


**Figure 4.** UV spectra of systems (A), (B). Schematic representation of possible supramolecular interaction of AT/ $\gamma$ CD/AA (C) and PEGXS-AT/ $\gamma$ CD/AA (D).

guest molecules, into AT/ $\gamma$ CD caused a blue shift for the Q/B peak, which is probably because AT molecules were pulled out from the cavities of  $\gamma$ CD by the interaction between  $\gamma$ CD and AA. Nevertheless, the Q/B peak of AT/ $\gamma$ CD/AA still exhibited a slight red shift compared with AT/ $\gamma$ CD, suggesting that not all of AT in the cavities was pulled out by AA (Figure 4(A) and (C)). The UV spectra of PEGXS-AT/ $\gamma$ CD and PEGXS-AT/ $\gamma$ CD/AA showed similar regulations with AT/ $\gamma$ CD and AT/ $\gamma$ CD/AA, respectively. The Q/B peak of PEGXS-AT/ $\gamma$ CD showed a red shift compared with PEGXS-AT, while the Q/B peak of PEGXS-AT/ $\gamma$ CD/AA showed a slight blue shift compared with PEGXS-AT/ $\gamma$ CD (Figure 4(B),(D)). It means that the supramolecular interaction between  $\gamma$ CD units with AT units still existed after AT segments grafted on the PEGXS polymer chain.

Both PEGXS-AT/ $\gamma$ CD<sub>2</sub> and PEGXS/ $\gamma$ CD<sub>2</sub> showed the sol-gel transition, indicating that there is a supramolecular interaction between  $\gamma$ CD units and PEGXS polymer backbone chains. In order to clarify the interaction between  $\gamma$ CD and PEGXS chain,  $\gamma$ CD instead of  $\gamma$ CD<sub>2</sub> was used to investigate the mechanism. Curves g and h in Figure 3 showed the <sup>1</sup>H NMR spectra of PEGXS-AT/ $\gamma$ CD and PEGXS/ $\gamma$ CD, respectively. Interestingly, the proton signals of  $\gamma$ CD in both PEGXS-AT/ $\gamma$ CD and PEGXS/ $\gamma$ CD became broader and shifted to a higher field. The changes are, of course, caused by the threading of the PEGXS polymer chain into  $\gamma$ CD cavities and the formation of the crystalline inclusion complex. Furthermore, the chemical shifts for H-3 and H-5 of  $\gamma$ CD for PEGXS-AT/ $\gamma$ CD shifted to a higher field than those for PEGXS/ $\gamma$ CD, which was mainly because  $\gamma$ CD units interacted with not only PEGXS segments but also AT segments in PEGXS-AT/ $\gamma$ CD (Figure 3 and Figure S10 in the Supporting Information). Moreover, when the excess amount of AA was added to the PEGXS-AT/ $\gamma$ CD and PEGXS/ $\gamma$ CD, the proton signals for H-3 and H-5 of  $\gamma$ CD shifted up higher than those for PEGXS-AT/ $\gamma$ CD and PEGXS/ $\gamma$ CD, respectively. These changes suggested that a stronger interaction took place between  $\gamma$ CD and AA, and PEGXS-AT and PEGXS polymer chains were pulled out from  $\gamma$ CD cavities.

X-ray diffraction patterns (XRD) and FT-IR analysis have been used to further investigate the structure of the inclusion complex formed by PEGXS polymer chains and  $\gamma$ CD units.

The patterns of PEGXS-AT/ $\gamma$ CD and PEGXS/ $\gamma$ CD are similar to other polymer/ $\gamma$ CD complexes which are known to possess column complexes, and the fingerprint peak for the column structure of the  $\gamma$ CD inclusion complex at ca. 7.5° was observed in both PEGXS/ $\gamma$ CD and PEGXS-AT/ $\gamma$ CD (Figure 5(A) and

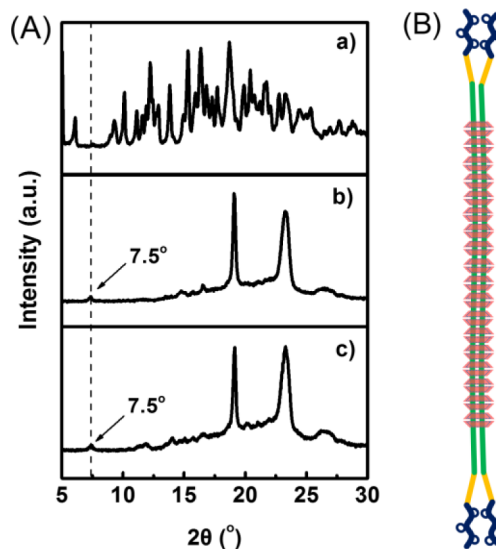


**Figure 5.** X-ray diffraction patterns of (a)  $\gamma$ CD, (b) PEGXS/ $\gamma$ CD, and (c) PEGXS-AT/ $\gamma$ CD (A). Schematic representation of the possible structure for PEGXS/ $\gamma$ CD (B).

Figure S13 in the Supporting Information).<sup>42–46</sup> In addition, a stoichiometry of 4:1 (ethylene glycol unit:  $\gamma$ CD) for PEG/ $\gamma$ CD was established in some reports to show that the complex contains two side-by-side PEG chains in each  $\gamma$ CD channel.<sup>43,45–48</sup> In this study, a stoichiometry of 8.2:1 (ethylene glycol unit:  $\gamma$ CD) was established for PEGXS/ $\gamma$ CD from <sup>1</sup>H NMR data (Figure S14 in the Supporting Information), suggesting that this complex not only contains two side-by-side PEG chains in each  $\gamma$ CD channel but also exhibits some part of “exposed” PEGXS polymer chains (Figure 5(B)). The absorption peak in FT-IR spectra between 3000 and 3500 cm<sup>-1</sup> is normally related to the hydroxyl groups (–OH stretch). The

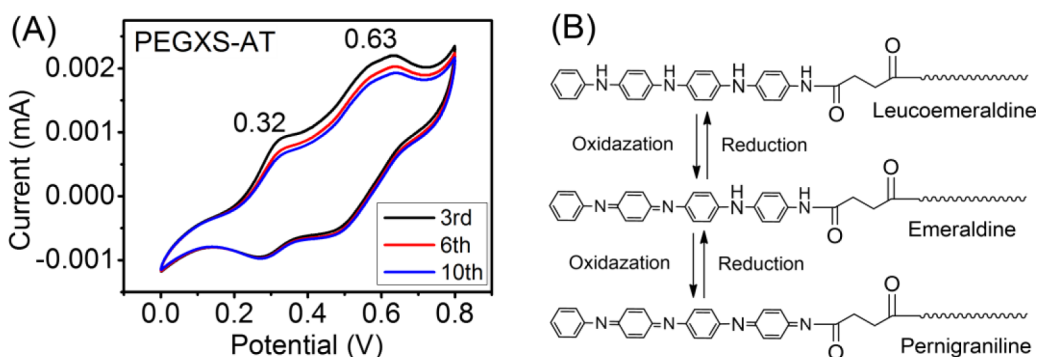


**Figure 6.** Cyclic voltammogram of PEGXS-AT in 1 M HCl aqueous solution with multiple cycles (A). Molecular structure of AT segments in PEGXS-AT copolymer in various oxidation states (B).

position of this absorbance band for pure  $\gamma\text{CD}_2$  is  $3308\text{ cm}^{-1}$ , and the peak shifted to higher frequency of  $3340\text{ cm}^{-1}$  when it forms the IC with the PEGXS-AT copolymer (Figure S15 in the Supporting Information). The shift of the  $-\text{OH}$  stretch is mainly due to the association of hydroxyl groups of  $\gamma\text{CD}$  and polymer chains, which agreed well with the interaction between  $\gamma\text{CD}$  and other copolymers in the literature.<sup>44</sup>

The electrochemical properties of this injectable electroactive hydrogel were investigated by cyclic voltammetry (CV) and UV spectra. There are two pairs of well-defined oxidation/reduction peaks appearing at 0.32 and 0.63 V for both PEGXS-AT and PEGXS-AT/ $\gamma\text{CD}_2$  in Figure 6(A) and Figure S16 in the Supporting Information, respectively. The peak at 0.32 V is assigned to the transition from the leucoemeraldine state to the emeraldine state. At the higher potential, 0.63 V, the peak suggests that the AT segment was oxidized from the emeraldine state to the pernigraniline state (Figure 6(B)). Moreover, the CV spectra of samples measured by multiple cycles also suggested that the electrochemical properties of these materials were stable. In addition, from the UV spectra of PEGXS-AT and PEGXS-AT/ $\gamma\text{CD}_2$  doped with 1 M HCl aqueous solution (Figure S12 in Supporting Information), it was observed that the  $\pi_{\text{B}}-\pi_{\text{Q}}$  excitonic transition peak at  $\sim 580\text{ nm}$  decreased. At the same time, the appearances of the polaron peaks at  $\sim 410\text{ nm}$  and the delocalized polaron peak at  $\sim 800\text{ nm}$  confirmed the generation of emeraldine salts (EMS) and the ability of conducting electrons of copolymer, which indicated both PEGXS-AT and PEGXS-AT/ $\gamma\text{CD}_2$  have the ability of electrical conducting. Therefore, the PEGXS-AT/ $\gamma\text{CD}_2$  shows similar CV and UV results with PEGXS-AT, which confirms that the interaction between  $\gamma\text{CD}$  and AT did not change the electrochemical properties of the PEGXS-AT copolymer. All these results from the UV and CV spectra demonstrated that the PEGXS-AT copolymer and PEGXS-AT/ $\gamma\text{CD}_2$  hydrogel have good electroactivity.

In summary, we successfully designed and synthesized a novel injectable electroactive hydrogel via supramolecular chemistry by host-guest interactions, which opens the new way to synthesize injectable conducting hydrogels to avoid the undesirable effect of covalent cross-linking. This hydrogel was simply achieved by using  $\gamma\text{CD}_2$  as the host molecule and PEGXS-AT copolymer as the guest component. The formation of injectable electroactive hydrogel is driven by host-guest interaction between the  $\gamma\text{CD}_2$  and aniline tetramer and poly(ethylene glycol). The injectable electroactive hydrogels obtained via noncovalent host-guest interactions offer numerous biomedical applications in various fields where the

electroactivity is in need, such as tissue engineering scaffolds, drug delivery systems, and biosensors.

## ■ ASSOCIATED CONTENT

### 📄 Supporting Information

Experimental procedure and additional data. This material is available free of charge via the Internet at <http://pubs.acs.org>.

## ■ AUTHOR INFORMATION

### Corresponding Authors

\*Tel.: +86-29-83395361. Fax: +86-29-83395131. E-mail: [baoling@mail.xjtu.edu.cn](mailto:baoling@mail.xjtu.edu.cn)

\*E-mail: [mapx@umich.edu](mailto:mapx@umich.edu).

### Notes

The authors declare no competing financial interest.

## ■ ACKNOWLEDGMENTS

The Natural Science Foundation of China (grant number: 21304073) was acknowledged for financial support of this work.

## ■ REFERENCES

- (1) Guo, B. L.; Glavas, L.; Albertsson, A. C. *Prog. Polym. Sci.* **2013**, *38*, 1263–1286.
- (2) Guimard, N. K.; Gomez, N.; Schmidt, C. E. *Prog. Polym. Sci.* **2007**, *32*, 876–921.
- (3) Li, L. C.; Ge, J.; Wang, L.; Guo, B. L.; Ma, P. X. *J. Mater. Chem. B* **2014**, *2*, 6119–6130.
- (4) Ma, X. J.; Ge, J.; Li, Y.; Guo, B. L.; Ma, P. X. *RSC Adv.* **2014**, *4*, 13652–13661.
- (5) Anderson, M. R.; Mattes, B. R.; Reiss, H.; Kaner, R. B. *Science* **1991**, *252*, 1412–1415.
- (6) Huang, J.; Virji, S.; Weiller, B. H.; Kaner, R. B. *J. Am. Chem. Soc.* **2003**, *125*, 314–315.
- (7) Bhadra, S.; Khastgir, D.; Singha, N. K.; Lee, J. H. *Prog. Polym. Sci.* **2009**, *34*, 783–810.
- (8) Guo, B. L.; Finne-Wistrand, A.; Albertsson, A.-C. *Macromolecules* **2010**, *43*, 4472–4480.
- (9) Huang, L. H.; Zhuang, X. L.; Hu, J.; Lang, L.; Zhang, P. B.; Wang, Y. S.; Chen, X. S.; Wei, Y.; Jing, X. B. *Biomacromolecules* **2008**, *9*, 850–858.
- (10) Guiseppi-Elie, A. *Biomaterials* **2010**, *31*, 2701–2716.
- (11) Guarino, V.; Alvarez-Perez, M. A.; Borriello, A.; Napolitano, T.; Ambrosio, L. *Adv. Healthcare Mater.* **2013**, *2*, 218–227.
- (12) Justin, G.; Guiseppi-Elie, A. *Biomacromolecules* **2009**, *10*, 2539–2549.
- (13) Green, R. A.; Hassarati, R. T.; Goding, J. A.; Baek, S.; Lovell, N. H.; Martens, P. J.; Poole-Warren, L. A. *Macromol. Biosci.* **2012**, *12*, 494–501.

- (14) Guo, B. L.; Finne-Wistrand, A.; Albertsson, A. C. *J. Polym. Sci., Polym. Chem.* **2011**, *49*, 2097–2105.
- (15) Guo, B. L.; Finne-Wistrand, A.; Albertsson, A. C. *Chem. Mater.* **2011**, *23*, 1254–1262.
- (16) Mawad, D.; Stewart, E.; Officer, D. L.; Romeo, T.; Wagner, P.; Wagner, K.; Wallace, G. G. *Adv. Funct. Mater.* **2012**, *22*, 2692–2699.
- (17) Runge, M. B.; Dadsetan, M.; Baltrusaitis, J.; Ruesink, T.; Lu, L. C.; Windebank, A. J.; Yaszemski, M. J. *Biomacromolecules* **2010**, *11*, 2845–2853.
- (18) Guo, B. L.; Finne-Wistrand, A.; Albertsson, A. C. *Biomacromolecules* **2011**, *12*, 2601–2609.
- (19) Zhang, L.; Li, Y.; Li, L.; Guo, B.; Ma, P. X. *React. Funct. Polym.* **2014**, *82*, 81–88.
- (20) Li, L. C.; Ge, J.; Guo, B. L.; Ma, P. X. *Polym. Chem.* **2014**, *5*, 2880–2890.
- (21) Kuijpers, A. J.; Engbers, G. H.; Krijgsveld, J.; Zaat, S. A.; Dankert, J.; Feijen, J. *J. Biomater. Sci. Polym. Ed.* **2000**, *11*, 225–243.
- (22) Speer, D. P.; Chvapil, M.; Eskelson, C.; Ulreich, J. *J. Biomed. Mater. Res.* **1980**, *14*, 753–764.
- (23) Nguyen, M. K.; Lee, D. S. *Macromol. Biosci.* **2010**, *10*, 563–579.
- (24) Liu, Y.; Hu, J.; Zhuang, X.; Zhang, P.; Wei, Y.; Wang, X.; Chen, X. *Macromol. Biosci.* **2012**, *12*, 241–250.
- (25) Dai, T.; Qing, X.; Lu, Y.; Xia, Y. *Polymer* **2009**, *50*, 5236–5241.
- (26) Yu, L.; Ding, J. *Chem. Soc. Rev.* **2008**, *37*, 1473–1481.
- (27) Harada, A. *Coord. Chem. Rev.* **1996**, *148*, 115–133.
- (28) Appel, E. A.; del Barrio, J.; Loh, X. J.; Scherman, O. A. *Chem. Soc. Rev.* **2012**, *41*, 6195–6214.
- (29) Zhang, J.; Ma, P. X. *Angew. Chem., Int. Ed.* **2009**, *48*, 964–968.
- (30) Zhang, J.; Ma, P. X. *Adv. Drug Delivery Rev.* **2013**, *65*, 1215–1233.
- (31) Huh, K. M.; Cho, Y. W.; Chung, H.; Kwon, I. C.; Jeong, S. Y.; Ooya, T.; Lee, W. K.; Sasaki, S.; Yui, N. *Macromol. Biosci.* **2004**, *4*, 92–99.
- (32) Deng, W.; Yamaguchi, H.; Takashima, Y.; Harada, A. *Angew. Chem.* **2007**, *119*, 5236–5239.
- (33) Liao, X.; Chen, G.; Liu, X.; Chen, W.; Chen, F.; Jiang, M. *Angew. Chem.* **2010**, *122*, 4511–4515.
- (34) Zhang, Z.; Liu, K. L.; Li, J. *Angew. Chem.* **2013**, *125*, 6300–6304.
- (35) Park, C.; Lee, K.; Kim, C. *Angew. Chem.* **2009**, *121*, 1301–1304.
- (36) Liu, K. L.; Zhang, Z.; Li, J. *Soft Matter* **2011**, *7*, 11290–11297.
- (37) Kretschmann, O.; Choi, S. W.; Miyauchi, M.; Tomatsu, I.; Harada, A.; Ritter, H. *Angew. Chem., Int. Ed.* **2006**, *45*, 4361–4365.
- (38) Tamesue, S.; Takashima, Y.; Yamaguchi, H.; Shinkai, S.; Harada, A. *Angew. Chem.* **2010**, *122*, 7623–7626.
- (39) Nakahata, M.; Takashima, Y.; Yamaguchi, H.; Harada, A. *Nat. Commun.* **2011**, *2*, 511.
- (40) Ali, S. M.; Upadhyay, S. K. *J. Incl. Phenom. Macrocycl. Chem.* **2008**, *62*, 161–165.
- (41) Yuan, G. L.; Kuramoto, N.; Takeishi, M. *Polym. Adv. Technol.* **2003**, *14*, 428–432.
- (42) Harada, A.; Okada, M.; Li, J.; Kamachi, M. *Macromolecules* **1995**, *28*, 8406–8411.
- (43) Harada, A.; Suzuki, S.; Okada, M.; Kamachi, M. *Macromolecules* **1996**, *29*, 5611–5614.
- (44) Lu, J.; Shin, I. D.; Nojima, S.; Tonelli, A. *Polymer* **2000**, *41*, 5871–5883.
- (45) Jiao, H.; Goh, S.; Valiyaveetil, S. *Macromolecules* **2002**, *35*, 1399–1402.
- (46) Jiao, H.; Goh, S.; Valiyaveetil, S. *Macromolecules* **2002**, *35*, 1980–1983.
- (47) Choi, H. S.; Ooya, T.; Lee, S. C.; Sasaki, S.; Kurisawa, M.; Uyama, H.; Yui, N. *Macromolecules* **2004**, *37*, 6705–6710.
- (48) Kawabata, R.; Katoono, R.; Yamaguchi, M.; Yui, N. *Macromolecules* **2007**, *40*, 1011–1017.